Chem Soc Rev

REVIEW ARTICLE

View Article Online
View Journal | View Issue

Cite this: *Chem. Soc. Rev.*, 2017, **46**, 2622

Assessing cooperativity in supramolecular systems†

Larissa K. S. von Krbek,‡[a] Christoph A. Schalley *[a] and Pall Thordarson *[b]

This tutorial review summarises different aspects of cooperativity in supramolecular complexes. We propose a systematic categorisation of cooperativity into cooperative aggregation, intermolecular (allosteric) cooperativity, intramolecular (chelate) cooperativity and interannular cooperativity and discuss approaches to quantify them thermodynamically using cooperativity factors. A brief summary of methods to determine the necessary thermodynamic data is given with emphasis on isothermal titration calorimetry (ITC), a method still underrepresented in supramolecular chemistry, which however offers some advantages over others. Finally, a discussion of very few selected examples, which highlight different aspects to illustrate why such an analysis is useful, rounds up this review.

Received 6th February 2017

DOI: 10.1039/c7cs00063d

rsc.li/chem-soc-rev

1 Introduction

As stated in Levinthal's famous paradox,[1] "if the as-synthesised unfolded polypeptide from the ribosome had to sample all possible conformations to fold into a protein, it would take longer than the age of the universe". In reality, this process is however completed within milliseconds, because of the cooperative interactions involved. Traditionally, cooperativity was defined narrowly around the interactions between substrate sites in allosteric enzymes (IUPAC Gold Book),[2] but it meanwhile took on a much broader meaning. Therefore, it can be redefined from a more thermodynamic perspective as:

[a] *Institut für Chemie und Biochemie, Freie Universität Berlin, Takustraße 3, 14195 Berlin, Germany. E-mail: christoph@schalley-lab.de; Fax: +49 30 838 4 52639; Tel: +49 30 838 52639*

[b] *School of Chemistry, The Australian Centre for Nanomedicine and the ARC Centre of Excellence in Convergent Bio-Nano Science and Technology, University of New South Wales, NSW 2052, Australia. E-mail: p.thordarson@unsw.edu.au; Fax: +61 2 9385 6141; Tel: +61 2 9385 4478*

† In memoriam Fritz Vögtle.

‡ Present address: Department of Chemistry, University of Cambridge, Lensfield Road, Cambridge, CB2 1EW, UK.

Larissa K. S. von Krbek

Larissa von Krbek received a Bachelor of Science degree in chemistry from the Freie Universität Berlin, Germany, in 2010, having completed a Bachelor thesis in the group of Prof. Dr Hans-Ulrich Reißig. In 2012, she obtained her Master's degree, working on multivalent supramolecular systems under supervision of Prof. Dr Christoph A. Schalley. She completed her PhD in chemistry at the Freie Universität Berlin in the group of Prof. Dr Christoph A. Schalley in 2016, continuing her work on the thermodynamic analysis of multivalent systems. Since 2017, she has been working as a postdoc in the group of Prof. Jonathan R. Nitschke at the University of Cambridge, UK.

Christoph A. Schalley

Christoph Schalley studied chemistry at the University of Freiburg/Germany and graduated in 1993 from the Technical University Berlin. In his PhD work with Helmut Schwarz at TU Berlin, he received his thorough education as a mass spectrometrist and gas-phase chemist. After postdoctoral work on supramolecular chemistry with Julius Rebek, Jr at The Scripps Research Institute, La Jolla/USA, he combined both topics when he started his own research group as a habilitand at the University of Bonn. In 2005, he was appointed professor of organic chemistry at Free University Berlin. The Schalley group's research topics are diverse and comprise supramolecular chemistry in the gas phase as well as in solution and at interfaces.

Cooperative processes are characterised by interactions or binding events involving multiple steps, where, compared to the first step, the free energy change (ΔG) in the subsequent interaction step(s) is either decreasing (positive cooperativity) or increasing (negative cooperativity). Conversely, in the absence of cooperative effects (non-cooperative systems), each step(s) is equal to the next one in energy.

The different facets of cooperativity as it pervades both biology[3] and chemistry[4–6] come in several guises (Fig. 1). Cooperative aggregation, including micelle formation, and intermolecular cooperativity, including host–guest complexation, essentially differ in terms of forming larger aggregates or discrete complexes. Intramolecular cooperativity includes the most spectacular example of cooperativity, the folding of a randomly configured polypeptide into a functional three-dimensional protein structure.[1] Interannular cooperativity is important in nature, *e.g.* when intramolecular protein folding is initiated and/or assisted by intermolecular binding of the unfolded peptide to a chaperone protein. This has recently been illustrated in an example of a self-chaperoning quaternary light-harvesting protein assembly.[6]

This tutorial review focuses on these four types of cooperativity in supramolecular chemistry – even though each one of them has its analogue in natural systems. We will first consider the important terms multivalency and allostery before describing cooperative homogeneous and heterogeneous aggregation. We will then move on to explaining the important issue of statistical factors before discussing three types of cooperativity in discrete non-covalent complexes. The simplest of these occurs in conventional host–guest complexes with monotopic (monovalent) guests – often referred to as allosteric cooperativity. The other two types are observed in multivalent systems that may exhibit intramolecular or chelate cooperativity and interannular cooperativity.

Pall Thordarson

Born on a farm in Vopnafjörður in the north-east of Iceland, Pall Thordarson (Palli) obtained his BSc degree from U. Iceland in 1996 and a PhD degree in Organic Chemistry from the University of Sydney, Australia in 2001 under the supervision of Maxwell Crossley. Following a Marie Curie Fellowship in the laboratory of Roeland Nolte and Alan Rowan at the University of Nijmegen, the Netherlands, he returned to the University Sydney in 2003 and was then appointed at the School of Chemistry UNSW in 2007 as a senior lecturer. He was promoted to a position of Full Professor in 2017. Palli's main research activities are currently focused on complexity in chemistry and functional nanomaterials, including light-harvesting dyes, self-assembled materials for nanomedicine, supramolecular equilibria and systems chemistry.

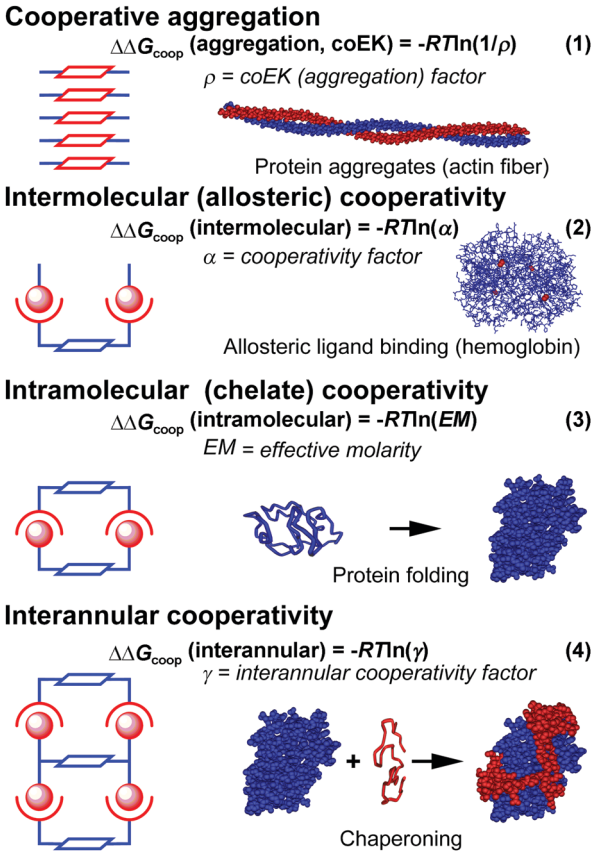

Fig. 1 The different facets of cooperativity in synthetic (left) and biological (right) systems. The energy difference between two subsequent binding events ($\Delta\Delta G_{coop}$ = difference between step n to step $n + 1$) associated with each type of cooperativity is also shown in eqn (1)–(4). See text for details.

In addition to describing the key features that define different forms of cooperativity, we will also describe the key methods required for its thermodynamic analysis and briefly discuss some of the most useful experimental techniques. We refer the reader to our earlier work for a more detailed description of the fundamentals of analysing binding data[7,8] and estimation of uncertainties,[9] including the key equations required to analyse simple host–guest equilibria. There are plenty of software solutions for determining binding energies or binding constants in simpler systems.[8] This includes accurate online-based tools for global data fitting for simple cooperative aggregation and 1 : 2 and 2 : 1 cooperative host–guest binding.[10] When dealing with more complex systems, researchers usually need to develop their own software solution to fit their data to the binding model they are investigating.

This review ends with the discussion of a few selected examples that illustrate the different aspects of supramolecular binding and aggregation that can be investigated using the concepts of cooperativity.

2 Multivalency

Many natural processes depend strongly on multivalent binding,[11,12] which we define as an interaction between a host/receptor and

a guest/ligand, both of which bear more than one binding site connected through spacers. Multivalency combines the advantages of reversibility and high binding strength in analogy to the Velcro® effect: a single hook does not carry much load and is easily released, but many together form a connection resisting even strong separation forces. One example is the docking of an influenza virus to its host cell.[11] It binds with homotrimeric hemagglutinin glycoprotein receptors to the sialic acids presented on the cell surface. Through many of these trivalent interactions, endocytosis of the virus is facilitated. As often the number of binding sites is not known in biological systems, the determination of cooperativity in the sense of our discussion below is not easily possible. Whitesides *et al.*[11] therefore defined the multivalent amplification or avidity factor β_{av} (eqn (5)), which relates the binding constant K_{multi} of the multivalent interaction to the monovalent binding constant K_{mono} of a single binding site.

$$\beta_{av} = \frac{K_{multi}}{K_{mono}} \quad (5)$$

Beyond biochemistry, multivalent interactions also offer advantages to supramolecular chemistry[12–14] – and this is not only because of an enhancement of binding strengths. By organising binding sites in space, the geometry of supramolecular complexes can be controlled. This consequently helps programming more complex assemblies with respect to stoichiometry and shape, including elaborated supramolecular coordination polymers.[15] In particular, the so-called multivalency effect usually ensures that discrete complexes rather than random oligomers are formed.

The latter aspect immediately raises the question, why the addition of spacers should result in the preferential formation of discrete complexes. As it appears, multivalent binding benefits from cooperativity effects that arise from the presence of spacers between the binding sites. Different models have been developed to explain this so-called chelate cooperativity in multivalent interactions. One model begins with the free host and guest. The first binding event between a multivalent host and a multivalent guest brings the other binding sites into close proximity. Thus, it increases their local concentrations and makes the following intramolecular binding events more likely to occur.[16] In contrast, the rebinding model[17,18] starts from the fully bound complex and argues with the probability of binding site dissociation and re-association between the fully and partly bound states of a multivalent complex. If one binding site of the fully bound complex dissociates, it remains in proximity to its interaction partner and is more likely to re-associate. The complex is kinetically ''trapped'' in its bound and partly bound states; complete dissociation becomes unlikely.

Clearly, the detailed investigation of cooperativity effects will contribute significantly to a profound understanding of the factors that govern multivalent binding. Besides the more practical issues indicated above, thermodynamic studies of multivalency and cooperativity will provide a profound understanding of cooperativity effects that is of fundamental importance for the design of multivalent supramolecular complexes.

3 Allostery – a comment

The concept of allostery deserves special attention, as it is a central concept in the field of cooperativity and simultaneously a source of debate and confusion. Traditionally, the Monod–Wyman–Changeux (MWC)[19] and Koshland–Némethy–Filmer (KNF)[20] allostery models described it as a binding event at one site that leads to a structural change at a distant site. In other words, a binding event is structurally transmitted to other vacant binding sites, increasing or decreasing binding affinity in subsequent binding steps.

The modern view in biophysics is much broader,[21,22] recognising that proteins and biomolecules are – under equilibrium conditions – an ensemble of dynamically interchangeable conformers, including in non-discrete biopolymers.[23] A binding event may therefore not influence (detectably) the structure of other distant binding sites, but by influencing these dynamics, shift the population of available conformers, making subsequent binding more or less favourable, thus resulting in the observed cooperativity in these systems. In smaller molecules, these effects could even be electronic, *e.g.* if binding on one site of a conjugated or aromatic bidentate receptor influences the opposite empty binding site through electron donating or withdrawing effects without any detectable structural changes.

The translation of this modern view from biochemistry to supramolecular chemistry is not as straightforward as it looks. The reason is that direct interactions between two monovalent guests on a divalent host, including through-space electrostatic interactions are sometimes the key source of cooperativity in smaller supramolecular systems, *e.g.* in the binding of sodium cations to simple bis-crown ethers.[24] In other words, there is no communication at all between the binding sites in the host. As an extreme example, one could also consider the ''binding'' of two protons (H^+) to a dibasic species, *e.g.*, diaminoalkanes or DABCO: if the two pK_a values differ significantly (as they do!), should this be classified as an allosteric interaction? Biochemistry researchers studying allostery have not considered this situation, but this has led to two opposing camps appearing in chemistry: on one side, there are those that take the view that all cooperative interactions that are not chelate interactions must be allosteric.[25] In the other camp, which has included one of us,[26] allostery requires some evidence of structural communication, in line with the classical MWC and KNF models.

We propose here that the term allostery might be reserved for those non-chelate cooperative interactions, where the spacer between the interaction sites appears to play a significant role. These interactions might be structural or much subtler dynamic, conformational or electronic effects. As the more general term which comprises the ''through-space'' as well as the ''through-spacer'' communication, we suggest ''intermolecular cooperativity'' in contrast to ''intramolecular cooperativity'' related to ring closure reactions (Fig. 1). As depicted at the bottom of Fig. 1, cases can occur in which both intermolecular and intramolecular cooperativity not only add up, but also interdepend on each other. These cases form the category of systems displaying ''interannular cooperativity'' as earlier defined by Schiaffino and Ercolani.[27]

4 Cooperative aggregation and supramolecular polymerisation

Micelles, gels, polymer nanoparticles and many other self-assembled systems are formed due to stabilising cooperative interactions between the molecules forming these aggregates. The thermodynamic description of these complex and mainly three-dimensional systems is beyond the scope of this work, however, simpler non-cyclic one-dimensional aggregates or supramolecular polymers,[28–30] are conceptually related to the discrete cooperative binding systems discussed below, and offer some useful insight into the fundamentals of cooperativity. We will briefly discuss this, including the difference between homogenous (one-component)[30] and heterogeneous (multi-component)[30] aggregation.

4.1 Homogenous aggregation

One-dimensional one-component homogenous aggregates are one of the simplest forms of supramolecular systems that may display cooperativity. Consider the linear aggregation of a molecule **A** into di-, tri-, tetra-…*i*-meric stacks of **A**. Using the terminology introduced by Martin,[31] we will only consider three cases here (Fig. 2): dimerisation, the equal K model (EK), also termed non-cooperative or isodesmic aggregation, where all the association constants are equal (K_E), and the cooperative equal K model (coEK), where the first association constant (K_2) differs from all the subsequent association constants (K_3, K_4, K_5…K_i) which are all equal – in other words, aggregation is cooperative once the initial dimer is formed.

The resulting binding equations and how they can be used with experimental NMR or UV-Vis dilution data have been described previously.[8,31] An online tool is available to fit data to these models.[10] The most important relation to consider is that between the first (monomer to dimer) and all subsequent equilibrium constants, for which the coEK cooperativity factor ρ is defined as $\rho = K_2/K_E$. If $\rho = 1$, the system is non-cooperative (Fig. 2). The definition of ρ is – likely for historical reasons – maybe somewhat counterintuitive as $\rho < 1$ stands for positive and $\rho > 1$ represents negative cooperativity. This is in marked contrast to the other cooperativity factors. The cooperativity factor ρ relates to the cooperativity-induced free energy difference $\Delta\Delta G_{coop}$ between the first and the subsequent aggregation step by eqn (6).

$$\Delta\Delta G_{coop} = -RT \ln \frac{1}{\rho} \quad (6)$$

It must be stressed here that eqn (6) only applies to the coEK aggregation model, and for each subsequent step in the coEK model $\Delta\Delta G_{coop} = 0$. There are many other aggregation models possible,[31] each would yield a different equation for the calculation of $\Delta\Delta G_{coop}$. It should also be noted that the aggregation cooperativity factor ρ is conceptually related to the cooperativity factor α (eqn (2)) discussed further below if one considers the relationship between $1/\rho$ and α in eqn (1) and (2) (Fig. 1).

Ercolani pointed out that the symmetry of the aggregating molecule is important. If the aggregating molecule has an *X*–*Y* symmetry, *i.e.*, it aggregates by forming an *X*–*Y*:(*X*–*Y*)$_n$:*X*–*Y* linear supramolecular polymer, then the statistical factor (σ, discussed further below),[3,32] for aggregation is $\sigma = 1$.[33] If the molecule has an *X*–*X* symmetry and aggregates by forming an *X*–*X*:(*X*–*X*)$_n$:*X*–*X* linear supramolecular polymer, then the statistical factor is $\sigma = 4$. Ercolani has also derived similar expressions for linear aggregation shown in Fig. 2,[33] pointing out the relationship between K_2 and dimerisation constant K_D, and showing on symmetry grounds that $K_2 = 2K_D$ in non-cooperative systems.

More importantly, Evstigneev and co-workers have unambiguously proved that non-cooperative aggregation and dimerisation are experimentally indistinguishable using conventional spectroscopic methods such as NMR or UV-Vis dilution studies.[34] That is, experimental data for such a system can fit equally well to a dimerisation *vs.* non-cooperative aggregation model. There are, however, situations where a dimer model can be selected on chemical grounds, *i.e.* when steric or electronic factors make the formation of higher-order aggregates (trimers, tetramers…) impossible. Alternative experimental approaches, including temperature-dependent isothermal calorimetry (ITC) measurements can also distinguish between the two models.[35]

As an alternative to dilution studies, temperature-dependent studies on aggregation equilibria can in some instances be used to extract the relevant thermodynamic quantities,[36,37] provided the interactions are reasonably strong and the spectroscopic signatures of the aggregates differ markedly from the monomer, *e.g.*, the circular dichroism (CD) signal from helical aggregates.[37] In principle, this approach could be used for the coEK model, but in the field of supramolecular polymer chemistry it is more common to deal with nucleation *vs.* elongation whereby nucleation is a slow step but might include more than two molecules. The relevant equations and methods for homogeneous supramolecular polymers have been described in detail previously.[36,37] When applicable, this method is highly advantageous as one temperature-dependent measurement on a single solution can yield all the data desired.

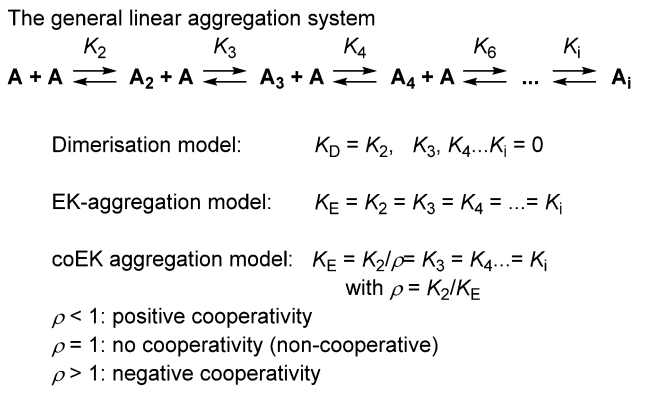

Fig. 2 Homogeneous (one-component) linear aggregation and the three most common binding models used to describe it (by convention in aggregation equilibria, the association constants are numbers 2, 3… according to the product stoichiometry in each step).

4.2 Heterogeneous aggregation

One-dimensional aggregation can also be heterogeneous (hetero-association), *i.e.*, if molecule **A** in Fig. 2 does not aggregate with itself,

but coaggregates with one or more similarly sized but different molecules **B** (hence sometimes referred to as multicomponent self-assembly).[30] In analogy to copolymerisation, the resulting aggregates could be block (**AAAABBBB**...), random (**AAABBAABBBAB**...), or alternating (**ABABABABAB**...) copolymers, with the latter being more common. Heterogeneous aggregates have a number of applications[38] ranging from fundamental studies on how (aromatic) drugs intercalate with DNA[39] to enhancing the solubility of poorly soluble aromatic drugs by the addition of other aromatic molecules (hydrotropes).[40]

It was pointed out in a recent comprehensive review on hetero-association by Evstigneev[34] that nearly all the models available to study heterogeneous aggregation, assume that it is non-cooperative. Notable exceptions include stochastic simulation algorithms[41–43] and mass-balance-based approaches[42,43] to evaluate cooperativity in heterogeneous aggregates. This includes temperature-dependent studies by Meijer and co-workers[42,43] on chiral aggregation involving two different enantiomers (*R* and *S*) of disk-shaped molecules and the study of the "sergeants-and-soldiers" and "majority-rules" principles in chiral amplification.

5 Discrete non-covalent complexes

Fig. 3 shows the three different types of cooperativity that can occur in discrete non-covalent complexes.[25,27] The first is intermolecular (or allosteric) cooperativity,[44,45] which can already occur in complexes assembled from monovalent guests and a multivalent host. The prototypical natural example is $\alpha_2\beta_2$ heterotetrameric haemoglobin (Fig. 1),[46] in which binding of the first O_2 molecule leads to a conformational change in the protein structure and higher binding strengths of the next ones. Intramolecular or chelate cooperativity[25,27] is the second type, which only occurs in complexes of a multivalent guest and a multivalent host. Chelate cooperativity is caused by connecting binding sites in both binding partners through suitable spacers and can be superimposed with additional effects from intermolecular cooperativity. The third type is interannular cooperativity,[27] which may occur when *e.g.* a first divalent component binds to a tetravalent one and preorganises the other two binding sites in a way that enhances or diminishes the binding strength of the second divalent component. Interannular cooperativity can be superimposed with intermolecular as well as chelate cooperativity effects.

5.1 Determining statistical factors

The assessment of cooperativity requires knowledge of the stepwise intrinsic binding constants (K_{i1}, K_{i2}...; Fig. 3, top row), which are related to the experimentally accessible apparent binding constants (K_1, K_2...) through statistical factors (σ, σ'...).[32]

A simple example: when a monovalent guest is offered two binding sites by a divalent host, it has a twice as high probability to bind as compared to the same guest binding to a monovalent host. Accordingly, the experimentally accessible apparent binding constant is thus twice as high – simply because of statistics. Similarly, the apparent binding constants for any of the other

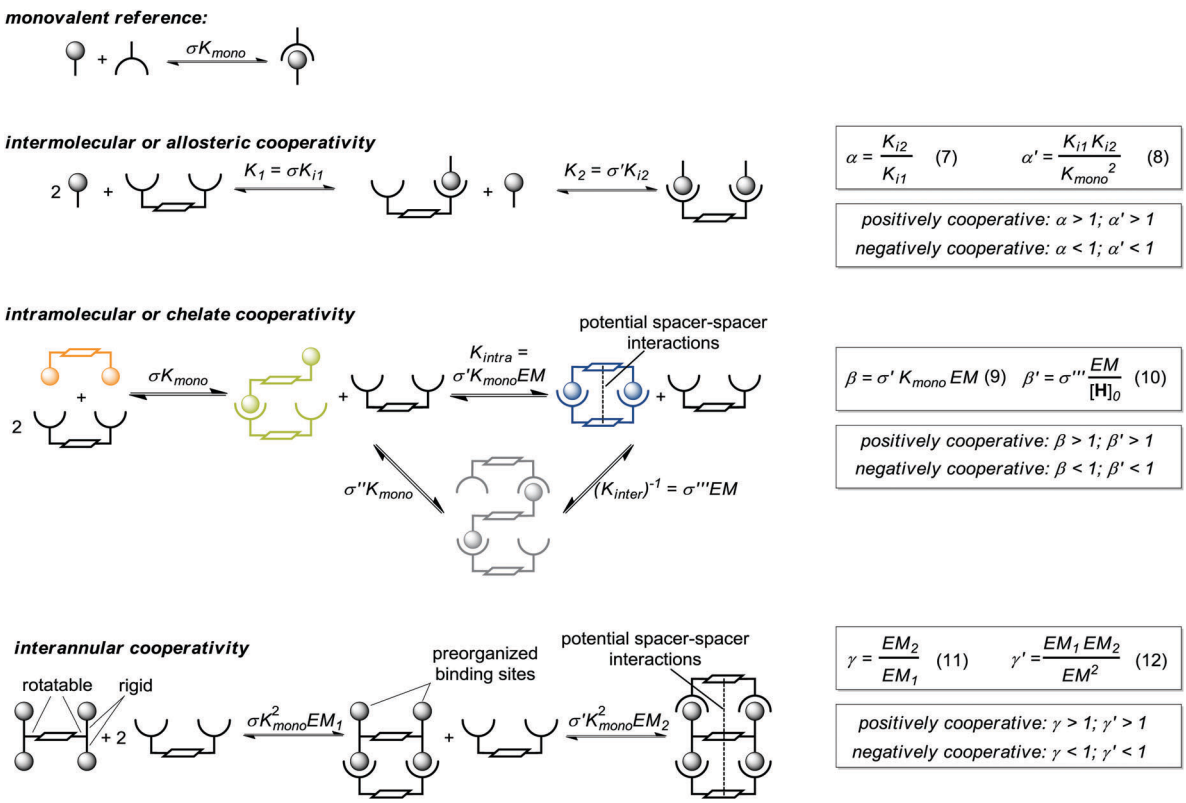

Fig. 3 The three types of cooperativity in discrete supramolecular complexes and the corresponding cooperativity factors.

individual binding steps shown in Fig. 3 can be deconvoluted into an intrinsic binding constant and a statistical factor.

For a precise analysis of cooperativity, the determination of statistical factors is thus important and two methods, the direct count method[47] and Benson's symmetry number method,[48] are most frequently used to determine them. The direct count method divides the number n_{prod} of the possible microspecies on the product side of an equilibrium by the number n_{react} of microspecies on the reactant side (eqn (13)).

$$\sigma = \frac{n_{\mathrm{prod}}}{n_{\mathrm{react}}} \tag{13}$$

For a correct determination of the number of microspecies, the binding sites – although chemically identical – must be considered as distinguishable. In, for example, the 1 : 2 allosteric system in Fig. 3 (second from top), the first monovalent guest can bind to either the left or the right binding site of the divalent host. Two microspecies are thus created as the product complexes ($n_{\mathrm{prod}} = 2$). On the reactant side, only free components exist, which count as one microspecies ($n_{\mathrm{react}} = 1$). Consequently, σ equals 2. In the second binding event, the second guest can bind only to the free binding site of the 1 : 1 complex. No matter to which of the two 1 : 1 microspecies the monovalent component binds, the 1 : 2 product microspecies will be the same. The product represents one microspecies, as there is only one "chemically plausible"[32] way to arrange them ($n_{\mathrm{prod}} = 1$). Consequently, σ' equals $\frac{1}{2}$.

In Benson's approach, the statistical factors σ are calculated from the product of all reactant symmetry numbers $\sigma_{i,\mathrm{react}}$ of the reactants divided by the product of all product symmetry numbers $\sigma_{i,\mathrm{prod}}$ of the products (eqn (14)).

$$\sigma = \frac{\prod_i \sigma_{i,\mathrm{react}}}{\prod_i \sigma_{i,\mathrm{prod}}} \tag{14}$$

$$\sigma_i = \sigma_{i,\mathrm{ext}} \cdot \sigma_{i,\mathrm{int}} \tag{15}$$

Each symmetry number σ_i is a product of an external and an internal symmetry number (eqn (15)). The external symmetry numbers $\sigma_{i,\mathrm{ext}}$ are derived from the point group of each species:

$$\sigma_{i,\mathrm{ext}} = 1 \quad \text{for } C_i,\ C_s,\ C_{\infty v},\ R_3$$

$$\sigma_{i,\mathrm{ext}} = 2 \quad \text{for } D_{\infty h}$$

$$\sigma_{i,\mathrm{ext}} = n \quad \text{for } C_n,\ C_{nv},\ C_{nh}$$

$$\sigma_{i,\mathrm{ext}} = 2n \quad \text{for } D_n,\ D_{nv},\ D_{nh}$$

$$\sigma_{i,\mathrm{ext}} = n/2 \quad \text{for } S_n \text{ (with even } n)$$

$$\sigma_{i,\mathrm{ext}} = 12 \quad \text{for } T_d$$

$$\sigma_{i,\mathrm{ext}} = 24 \quad \text{for } O_h$$

$$\sigma_{i,\mathrm{ext}} = 60 \quad \text{for } I_h$$

The internal symmetry numbers $\sigma_{i,\mathrm{int}}$ arise from internal rotations around single bonds, in other words different possible conformers. These conformational changes are usually fast as compared to the time scale of the association processes and can therefore be neglected.[32] Applying these considerations to the schematic guests and hosts in the equilibrium in Fig. 3 (second from top) results in the following statistical factors: on the reactant side, a product of symmetry numbers of 2 is obtained (free guest: $C_{\infty v} \rightarrow \sigma_{\mathrm{ext}} = 1$; free host: $C_{2v} \rightarrow \sigma_{i,\mathrm{ext}} = 2$). After the first binding event, the 1 : 1 complex has C_s symmetry ($\sigma_{\mathrm{ext}} = 1$) and together with the second free guest, the product of symmetry numbers is 1. The statistical factor for the first step is consequently $\sigma = 2$. The final 2 : 1 complex has a symmetry number of $\sigma_{\mathrm{ext}} = 2$ (C_{2v}), so that $\sigma' = \frac{1}{2}$. Both methods thus lead to the same results and either one can be used to crosscheck the statistical factors obtained using the other.

The tetravalent guest in Fig. 1 (bottom) represents a special case, in which completely neglecting internal symmetry numbers will lead to wrong statistical factors. Here, the possibility to freely rotate one pair of binding sites with respect to the other increases the number of possible host–guest interactions. Hence, this internal rotational flexibility of the guest around an internal C_2 axis, which only exists in the free guest, needs to be accounted for by an internal symmetry number of $\sigma_{\mathrm{int}} = 2$.

Once, the statistical factors are known, the intrinsic binding constants can be determined for each binding event from the experimentally accessible ones.

5.2 Quantifying intermolecular cooperativity

For a 1 : 2 complex of a divalent host and two monovalent guests K_{i1} and K_{i2} are the intrinsic, statistically corrected binding constants of the two subsequent binding steps (Fig. 3, second from top). Intermolecular cooperativity is present, if $K_{i1} \neq K_{i2}$. In a non-cooperative case, the two intrinsic binding constants are equal and (ideally) identical to that of a monovalent reference complex (K_{mono}). The same analysis holds true for the intrinsic binding constants of a 2 : 1 complex of two monovalent hosts and a divalent guest. As the divalent component is different in these two cases, also the intermolecular cooperativity effects differ from each other for the 1 : 2 *vs.* 2 : 1 complexes.

In order to quantify allosteric cooperativity, two slightly different cooperativity factors can be defined as shown in Fig. 3 (eqn (7) and (8)). The first factor α relates both intrinsic binding constants to each other, while α' relates K_1 and K_2 to the monovalent reference complex. Both factors indicate non-cooperative binding, when they are equal to one. Positive intermolecular cooperativity is observed for factors $\alpha > 1$ and $\alpha' > 1$, respectively. Here, the first binding event enhances binding at the second site. If $\alpha < 1$ and $\alpha' < 1$, negative cooperativity is encountered and binding the first guest reduces the affinity of the second. It should be noted that only in an ideal situation, in which the first binding event at the divalent host is not affected by the unavoidable structural differences between the spacered divalent and the non-spacered monovalent host, K_{i1} equals the binding constant for the monovalent reference complex K_{mono} – and thus $\alpha = \alpha'$. As the spacer usually has at least a small effect on the first binding event, a comparison of K_{i1} and K_{mono} is often useful to determine how large these effects and how innocent the

spacers really are. Analogous considerations can be applied to complexes of higher valency.

The cooperativity factor α is related to the cooperativity-induced free energy difference between the first and the second binding step. We should keep in mind, however, that α is derived from the intrinsic binding constants that are corrected for statistical factors. To link it to the macroscopically measurable $\Delta\Delta G$, it is therefore important to take into account the statistical factors appropriately (eqn (16) and (17)).

$$\Delta\Delta G = -RT\ln\frac{\sigma' K_{i2}}{\sigma K_{i1}} = \Delta\Delta G_{\text{stat}} + \Delta\Delta G_{\text{coop}} \quad (16)$$

$$\Delta\Delta G = -RT\ln\frac{\sigma'}{\sigma} - RT\ln\frac{K_{i2}}{K_{i1}} = -RT\ln\frac{\sigma'}{\sigma} - RT\ln\alpha \quad (17)$$

5.3. The effective molarity and intramolecular cooperativity

When describing the binding of a divalent host to a divalent guest (Fig. 3, centre), again two binding events occur. In contrast to the formation of the 1 : 2 complex in Fig. 3 (second from top), the second step now occurs intramolecularly. A 1 : 1 complex is formed, resulting in an overall binding constant K_{tot} with the unit M^{-1}. If one wishes to express K_{tot} in terms of K_{mono} (and of course the correct statistical factors), the unit would however be M^{-2} as K_{mono} appears in the equilibrium constants of both individual binding steps (eqn (18)).

$$K_{\text{tot}} = \sigma K_{\text{mono}} \sigma' K_{\text{mono}} \text{EM} \quad (18)$$

Obviously, a correction factor is required, which accounts for the intramolecular nature of the second binding step. This factor is called effective molarity EM. As expressed in eqn (18), it has the unit of concentration and was originally introduced into the rate laws of kinetically controlled covalent ring formation reactions.[49] This concept can, however, easily be transferred to the usually thermodynamically controlled supramolecular complex formation reactions. EM is then a thermodynamic quantity and is the crucial parameter for determining the threshold concentration, at which a di- or multivalent complex opens and forms oligomers (see below).

The equilibria shown in Fig. 3 (centre) are based on the assumption that the total host concentration $[\mathbf{H}]_0$ is significantly larger than the total guest concentration $[\mathbf{G}]_0$. Under these conditions, we can assume that also the 2 : 1 oligomer (grey) forms, but no 1 : 2 oligomers or longer chains. All four equilibrium constants can then be expressed based on K_{mono}, the corresponding statistical factors and the effective molarity.

Two ways to quantify intramolecular cooperativity are also shown in Fig. 3 (eqn (9) and (10)). Anderson and Hunter[25] used the equilibrium between the open (green) and the closed 1 : 1 complex (blue). When the concentration of both complexes is equal, K_{intra} is 1. Positive intramolecular cooperativity would shift the equilibrium towards the closed complex, and negative intramolecular cooperativity towards the open complex. Therefore, the first cooperativity factor β (Fig. 3, eqn (9)) can be defined as the product of statistical factor σ', the monovalent reference binding constant K_{mono} and the effective molarity EM (actually, the definition of β used by Anderson and Hunter neglects the statistical factor as it is small in most cases).

This approach has been criticised because the cooperativity factor now depends on K_{mono}, which implies that multivalent binding strength enhancements depend on the strength of the chosen binding motif. Therefore, Ercolani and Schiaffino defined a second intramolecular cooperativity factor β' (Fig. 3, eqn (10)) which is based on the equilibrium between the closed divalent complex and the free host on one side and the 2 : 1 oligomer on the other. As changes in the concentration of the host will cause a shift of the equilibrium in addition to an intramolecular cooperativity effect, this equilibrium constant is normalised by the host concentration. One should note that an approximation is made for practicability when using the total host concentration $[\mathbf{H}]_0$ here instead of the actual host concentration $[\mathbf{H}]$. Strictly speaking, this approximation is only valid in the presence of a large excess of the host – a situation which is rather far from the typical experimental conditions.

Both intramolecular cooperativity factors thus have their advantages and disadvantages. However, in our own experience, both of them are useful for quantifying intramolecular cooperativity. So far, we have not encountered a case in which both factors would result in contradicting cooperativity trends.

Unfortunately, it is not straightforward to link β or β' to the cooperativity-induced free energy difference $\Delta\Delta G$ between the first and the second binding step. Instead, the overall $\Delta\Delta G$ can be deconvoluted into a $\Delta\Delta G_{\text{stat}}$ derived from the statistical factors and a term $\Delta\Delta G_{\text{coop}}$ related to the effective molarity EM (eqn (19) and (20)).

$$\Delta\Delta G = \Delta\Delta G_{\text{stat}} + \Delta\Delta G_{\text{coop}} \quad (19)$$

$$\Delta\Delta G = -RT\ln\frac{\sigma' K_{\text{mono}}\text{EM}}{\sigma K_{\text{mono}}} = -RT\ln\frac{\sigma'}{\sigma} - RT\ln\text{EM} \quad (20)$$

Fig. 4 shows two speciation profiles, which demonstrate the effects of intramolecular cooperativity. As expected, there is virtually no doubly bound complex (blue line) formed in the absence of intramolecular cooperativity ($K_{\text{intra}} = \beta = 0$; left plot). The open complex (green line) is only present as an intermediate until the total host concentration $[\mathbf{H}]_0$ is high enough for oligomer formation (grey line). In marked contrast, the presence of a strong intramolecular cooperativity ($K_{\text{intra}} = \beta = 25$; right plot) suppresses

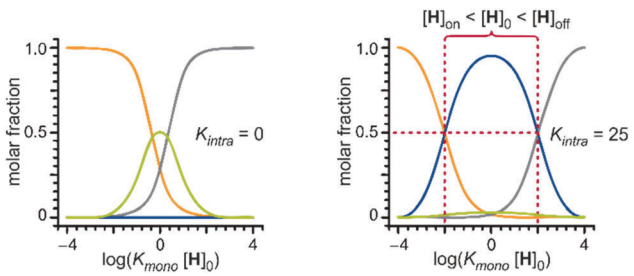

Fig. 4 Speciation profiles in the absence of chelate interaction ($K_{\text{intra}} = 0$; left) and in the presence of a strong chelate interaction ($K_{\text{intra}} = 25$; right). The lines are coded with the same colours as the complexes shown in Fig. 3 (centre).

the intermediate open complex and oligomerisation occurs at a much higher host concentration $[\mathbf{H}]_0$. Most importantly, there is a concentration-dependent "all-or-none" effect observed for the doubly bound complex: at medium host concentrations, the doubly bound complex suppresses all other species. Instead, at very low or very high host concentrations, the unbound guest (orange line) or oligomers (grey line) are favoured, respectively.

When the binding constants are known, the concentration $[\mathbf{H}]_{on}$ at which the divalent complex begins to dominate over the free guest can be calculated. Here, the concentrations of the closed divalent complex [**C**] and the free guest [**G**] are equal, and based on the overall binding constant K_{tot} (eqn (21)) one obtains eqn (23) as an expression of the lower threshold concentration for divalent complex formation:

$$K_{tot} = \frac{[\mathbf{C}]}{[\mathbf{G}][\mathbf{H}]} = \sigma\sigma'(K_{mono})^2 EM \quad (21)$$

$$\frac{[\mathbf{C}]}{[\mathbf{G}]} = \sigma\sigma'(K_{mono})^2 EM[\mathbf{H}]_{on} = 1 \quad (22)$$

$$[\mathbf{H}]_{on} = (\sigma\sigma'(K_{mono})^2 EM)^{-1} \quad (23)$$

At the upper limit, at which oligomers start to dominate, the ratio of oligomer to closed divalent complex is 1 and $[\mathbf{H}]_{off}$ can be calculated similarly:

$$[\mathbf{H}]_{off} = (K_{inter})^{-1} = \sigma'' EM \quad (24)$$

Between these two concentrations, the closed divalent complex is the most dominant species present. When determining thermodynamic data, care should be taken that the study is conducted within this concentration range, in particular when using non-structure-sensitive methods such as isothermal titration calorimetry.

The discussion here restricts itself to the question of cyclization *vs.* polymerization[50] of divalent systems and how intramolecular cooperativity greatly contributes to the formation of discrete complexes. This can be extended to much more complicated supramolecules such as hydrogen-bonded or metallosupramolecular self-assembled cages and capsules – however at the price that many cyclization reactions occur, each one with its own effective molarity. This makes the analysis more complicated. An alternative and simpler thermodynamic model has been given by Hamacek *et al.*[51–53]

5.4 Determination of effective molarities: double mutant cycles

The crucial question for a thermodynamic analysis of intramolecular cooperativity is now how the effective molarity can be determined. As the intermolecular cooperativity effects observed in 2 : 1 and 1 : 2 complexes may well affect also the binding in a divalent complex, it is important to determine EM in a way unaffected by them. To achieve this, the double mutant cycle analysis originally introduced by Jencks[54] provides a suitable tool (Fig. 5, top).[55] Two mutations are introduced into the divalent complex **A**: the first mutation corresponds to dissecting the spacer of the divalent host and leads to the 2 : 1 complex **B**.

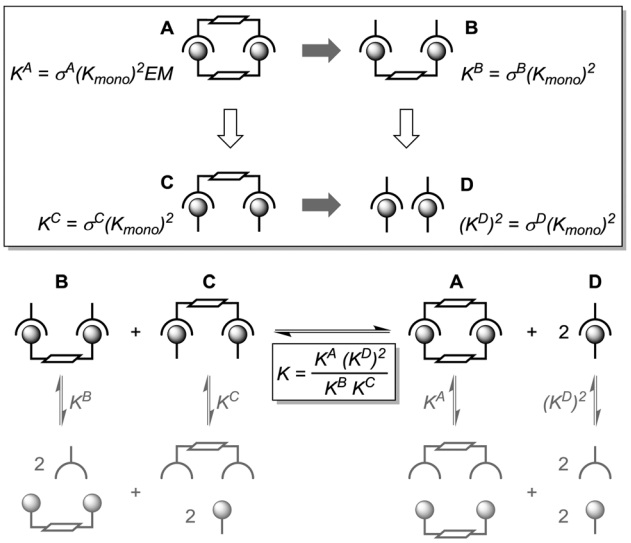

Fig. 5 Top: Double mutant cycle. Mutation 1 corresponds to a cut through the spacer of the host and mutation 2 to a cut through the spacer of the guest. Bottom: Equilibrium between complexes **A**, **B**, **C** and **D**. The equilibrium constant can be expressed by the four experimentally accessible equilibrium constants K^A, K^B, K^C, and K^D, which again correspond to expressions containing only statistical factors, the monovalent reference constant K_{mono} and the effective molarity EM.

The second mutation, *i.e.* dissecting the spacer of the divalent guest, leads to the 1 : 2 complex **C**. Finally, both mutations applied simultaneously lead to **D**. For all four complexes, the association constants can be determined experimentally, and all four can be expressed by statistical factors, the monovalent reference constant and EM. Note that the monovalent complex is formed twice when both mutations are applied. Therefore, K^D appears squared here.

If one now considers the equilibrium in Fig. 5 (bottom), which is derived from the double mutant cycle, the advantages of the double mutant cycle analysis become clear. First, all components appear on both sides of the equilibrium with an identical number of copies. Consequently, all intermolecular cooperativity effects appear on both sides of the equilibrium and thus cancel. The second advantage is that only four experimental measurements of the individual binding constants K^A, K^B, K^C and K^D allow us to determine not only the intermolecular effects as discussed above, but also EM and with it chelate cooperativity. When these four binding constants are known, the overall binding constant K can be calculated (eqn (25)):

$$K = \frac{K^A (K^D)^2}{K^B K^C} = \frac{\sigma^A {K_{mono}}^2 EM \sigma^D {K_{mono}}^2}{\sigma^B {K_{mono}}^2 \sigma^C {K_{mono}}^2} = \frac{\sigma^A \sigma^D}{\sigma^B \sigma^C} EM \quad (25)$$

$$EM = \frac{\sigma^B \sigma^C}{\sigma^A \sigma^D} K \quad (26)$$

It can also be expressed based on K_{mono} by inserting the expressions for the four individual constants given in Fig. 5. As all monovalent binding constants cancel in this equation, the effective molarity can very simply be calculated from the overall equilibrium constant K and the statistical factors (eqn (26)).

5.5 Interannular cooperativity

Interannular cooperativity[27] arises from the interplay of two or more chelating interactions on one multivalent component. The interactions affect each other in an allosteric fashion. A simple example is schematically shown in Fig. 3 (bottom). The association of the first divalent host with the tetravalent guest freezes its internal rotors and thus facilitates the association of the second divalent guest as the two binding sites are now preorganised. Both binding steps are ring closure reactions and therefore associated with two effective molarities, EM_1 for the first and EM_2 for the second ring-closing step.

In analogy to the intermolecular cooperativity factors α and α', interannular cooperativity effects can be quantified by comparing the two effective molarities EM_1 and EM_2 either with each other or with the effective molarity EM of a divalent reference system. Consequently, two different cooperativity factors γ and γ' can be defined (Fig. 3, eqn (11) and (12)).

Like the above relation between α and α', γ is equal to γ' in the ideal case that $EM_1 = EM$, which means that the first ring closure reaction is not affected by the two additional binding sites and the spacer connecting them to the backbone. Again, positive cooperativity is expressed when these factors are larger than 1; negative cooperativity is indicated when they are smaller than one. As mentioned above, the effective molarities can be determined by suitable double mutant cycle analyses. The analogy between the two cooperativity factors α and γ is also expressed by the fact that γ can again be related to the cooperativity-induced free energy difference $\Delta\Delta G$ of the two binding steps (eqn (27)).

$$\Delta\Delta G = \Delta\Delta G_{stat} + \Delta\Delta G_{coop} = -RT\ln\frac{\sigma'}{\sigma} - RT\ln\gamma \qquad (27)$$

Although a few examples exist,[56–58] which might exhibit interannular cooperativity, to the best of our knowledge, it has never been investigated in detail so far.[27]

6 Methods for thermodynamic analyses of cooperativity

Choosing the right experimental technique to determine the thermodynamic parameters of interest (K_i, ΔG...) is not a straightforward task, even for relatively simple systems where cooperativity plays a role. As outlined in previous reviews,[7–9] experimental scientists should aim to pick technique(s) that fit the concentration range that corresponds to the biggest changes in the equilibria under investigation. The measured physical property (Y) should ideally be highly sensitive to these equilibria. Practical issues such as the quantity of material required, speed and cost do of course also matter. High-throughput methods are particularly useful as they enable researchers to perform more repeat experiments and screen a larger library of reference compounds – in both cases significantly improving the accuracy of the thermodynamic parameters being sought. With this in mind, we will briefly review again the most commonly used supramolecular titration methods; NMR, UV-Vis, CD and fluorescence spectroscopy and then explain in more detail isothermal titration calorimetry (ITC), which is often overlooked, but particularly useful when studying the complex equilibria discussed here.

6.1 NMR titration experiments

The most popular method for supramolecular titration studies is (^{1}H) NMR. It needs to be remembered that it does not work for systems with large association constants, *e.g.* in the case of 1 : 1 complexation, it is generally unsuitable for $K > 10^5$ M^{-1}.[7–9] For the intramolecular chelate systems discussed above, it can be similarly problematic as these interactions are often in the slow exchange region. It is, however, useful for simpler cooperative systems and in many cases ideal for the study of 1 : 2 allosteric binding.

In 1 : 2 equilibria, NMR titration studies can reveal even very subtle structural effects of the first binding event on the other binding site(s).[59] Provided the stepwise macroscopic binding constants are not too big ($\approx < 10^5$ M^{-1} each), quantitative information is obtained by fitting the titration data to the (differential) binding isotherms (eqn (28)). This model involves the two binding macroscopic binding constants K_1 and K_2 and two differential NMR proton resonances $\delta_{\Delta HG_2}$ ($=\delta_{\Delta HG_2} - \delta_{HG}$) and $\delta_{\Delta HG}$ ($=\delta_{HG} - \delta_H$) and the free concentration of the guest [G] obtained from a cubic equation described previously (eqn (28)).[7,8]

$$\Delta\delta = \frac{\delta_{\Delta HG}K_1[G] + \delta_{\Delta HG_2}K_1K_2[G]^2}{1 + K_1[G] + K_1K_2[G]^2} \qquad (28)$$

The accuracy of K_1 and K_2 can be further enhanced by global analysis[7–9,60] methods monitoring simultaneously the changes in more than one resonance as the titration progresses. In terms of studying cooperative aggregation, NMR dilution studies are usually the method of choice[8,31] as their dynamic range is typically larger than UV-Vis studies that are based on relatively small deviations from the Beer–Lambert law.

6.2 UV-Vis, CD and fluorescence spectroscopy experiments

For complex equilibria, while inferior in terms of structural information when compared to NMR methods, UV-Vis titration experiments can be quite useful for thermodynamic analyses.[61] This is because much larger equilibrium constants can be obtained than those possible by NMR. With a suitable chromophore, micromolar concentrations can be used. This has two advantages in that oligomeric species are largely suppressed and hence data analysis is simplified in chelate cooperativity and in that the implicit assumption of ideal solutions (activity coefficients all equal to 1) made in nearly all the models used in these studies is more realistic. The ease of UV-Vis and modern plate reader technologies has also enabled high throughput UV-Vis methods for the study of cooperative systems.[62]

Circular dichroism (CD) spectroscopy is a particularly powerful method for investigating cooperativity in chiral supramolecular polymers. As previously mentioned, CD spectroscopy can be used to obtain detailed data on the chiral aggregation in a single

temperature-dependent measurement as shown in numerous studies by Meijer.[36,37,42,43,63]

In analogy to UV-Vis studies, fluorescence spectroscopy is another powerful method for the investigation of cooperative interactions that are much larger than those accessible by NMR. Fluorescence spectroscopy has for instance been used to investigate cooperativity in 1 : 2 host–guest systems[59,64] and *via* temperature-dependent methods to differentiate pre-aggregates from aggregates in the cooperative aggregation of π-conjugated supramolecular polymers.[37]

6.3 Isothermal titration calorimetry

One of the most convenient methods is isothermal titration calorimetry (ITC). As this method is not as frequently used in supramolecular chemistry, although it offers a number of advantages, we will discuss it here in more detail. ITC delivers the association stoichiometry n, the association constant K and with it the Gibbs free association energy ΔG, the association enthalpy ΔH and the association entropy ΔS of the system under study in one single measurement while offering a large dynamic range up to K values of 10^9 M^{-1}.[65–67] Hence, ITC exceeds other techniques in information density. Detailed insights into the thermodynamics of supramolecular interactions, not only dimeric, but also supramolecular polymeric interactions,[67] as well as their cooperativities can be gained. ITC, as a calorimetric technique, measures the heat change occurring during an association reaction directly and non-invasively. As a drawback, it provides no information about the nature of the processes causing the heat changes at the molecular level. Hence, ITC should always be combined with complementary techniques capable of delivering this information.

An ITC instrument consists of a twin-calorimeter set-up of a sample and a reference cell (Fig. 6, left). Any thermal event in the sample cell is measured as a differential signal from the reference cell (Q_s: heat development in the sample cell; T_s, T_r: temperatures in sample and reference cell, C: heat capacity of the sample; k: heat transfer coefficient; eqn (29)).[68]

$$\frac{dQ_s}{dt} = k(T_s - T_r) \tag{29}$$

In a typical titration experiment, the sample cell contains a solution of one of the interacting components (usually the host). The reference cell contains blank solvent. A small amount of a more concentrated solution of the second interaction partner (the guest) is titrated into the sample cell. After each addition of guest solution, the following host–guest complex formation generates a thermal event resulting in a heat flow signal (Fig. 6, top right). A time delay between the titration steps allows the system to re-equilibrate before the next injection. The heat evolved or absorbed by the reaction is calculated by integration of the heat flows of each titration peak and plotted against the molar ratio of the host and guest providing the binding isotherm (Fig. 6, bottom right). The isotherm is described by the following equation, the so-called Wiseman isotherm[69,70] (V_0: effective cell volume; $[G]_t$, $[H]_t$: concentration of guest and host after titration step t):

$$\frac{dQ_s}{d[G]_t} = \frac{\Delta H V_0}{2}\left(1 + \frac{1 - \frac{[G]_t}{[H]_t} - \left(K_a[H]_t\right)^{-1}}{\sqrt{\left(1 + \frac{[G]_t}{[H]_t} + \left(K_a[H]_t\right)^{-1} - 4\frac{[G]_t}{[H]_t}\right.}}\right) \tag{30}$$

Non-linear curve fitting of the isotherm according to eqn (30) yields three parameters in one measurement: (a) the complex stoichiometry n as the molar ratio of the host and guest at the isotherm's inflection point (orange), (b) K_a from the isotherm's slope at the inflection point (green) and (c) ΔH from the step height of the isotherm (blue).[69,70] ΔG is easily calculated from K_a ($\Delta G = -RT\ln K_a$), ΔS from ΔG and ΔH ($\Delta G = \Delta H - T\Delta S$).

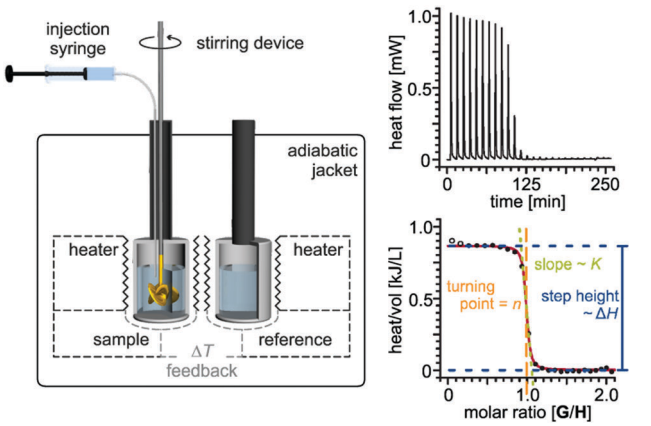

Fig. 6 Left: Schematic representation of an isothermal titration calorimeter. Right: Typical titration curve of an exothermic association measured on a heat-conduction calorimeter (top) and the corresponding binding isotherm plot of integrated heat flows against the molar ratio. Orange, green, and blue marks indicate how the thermodynamic parameters n, K, and ΔH are obtained. ΔG and ΔS can be calculated from K and ΔH.

7 Selected examples

Emergence is the idea that the whole is more than the sum of its parts and as cooperative interactions are by definition non-linear, it is an excellent tool to study emergent properties and create unusual structures in supramolecular chemistry. Using – a few out of many more – illustrative examples, this section demonstrates the different types of cooperativity discussed in this review.

7.1 Aggregation

Studies on 1,2,4,5-tetra(ethylhexanoate)pyromellitamide (Fig. 7a) showed that this molecule readily forms organogels in non-polar solvents such as cyclohexane. In more polar acetone, gelation is not observed, but clear evidence of aggregation is obtained from NMR dilution studies. The data were fitted to dimerisation, non-cooperative and coEK aggregation models (Fig. 2). As predicted by Evstigneev,[34] the data fitted equally,[8,71] albeit badly to the non-cooperative and dimerisation models. A much better fit was obtained using the coEK model with $K_2 = 51$ M^{-1} and $K_E = 232$ M^{-1}, corresponding to positive cooperativity with

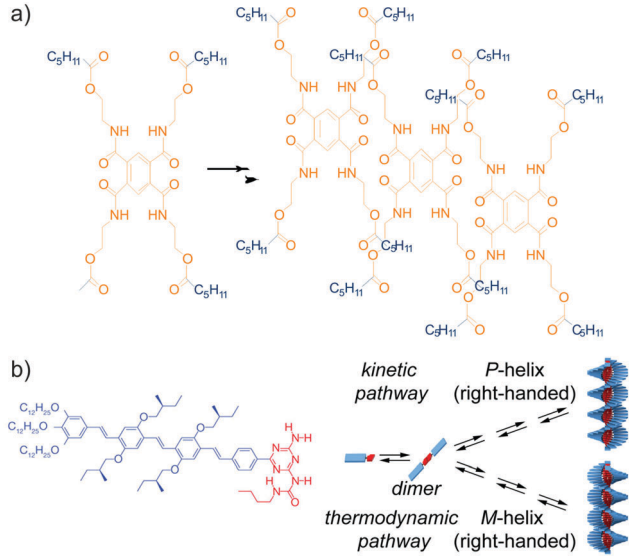

Fig. 7 Two examples of cooperative aggregation. (a) The structure of 1,2,4-5-tetra(ethylhexanoate)pyromellitamide (left) that forms aggregates (right) in acetone with the data fitting to the cooperative coEK model with K_E = 232 M^{-1} and ρ = 0.22.[71] (b) The *S*-chiral oligo(*p*-phenylenevinylene) on the left can aggregate to form either the thermodynamically stable left handed (*M*) or a metastable right-handed (*P*) helix.[63] (b) is adapted from ref. 63 with kind permission by MacMillan Publishers.

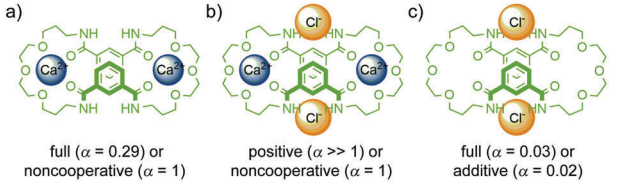

d)

	relationship between	
binding model	K_1 and K_2	$\delta_{\Delta HG}$ and $\delta_{\Delta HG_2}$
statistical 1:2	$K_1 = 4K_2$	$\delta_{\Delta HG_2} = 2\delta_{\Delta HG}$
noncooperative 1:2	$K_1 = 4K_2$	$\delta_{\Delta HG_2} \neq 2\delta_{\Delta HG}$
additive 1:2	$K_1 \neq 4K_2$	$\delta_{\Delta HG_2} = 2\delta_{\Delta HG}$
full 1:2	$K_1 \neq 4K_2$	$\delta_{\Delta HG_2} \neq 2\delta_{\Delta HG}$

Fig. 8 Different 1 : 2 binding models and cooperativity in a tetratopic ion-pair receptor bound to (a) two calcium (Ca^{2+}), (b) two chloride (Cl^-) and two calcium (Ca^{2+}) and (c) two chloride (Cl^-) ions. Shown below the structures in (a)–(c) are the results based on the best fit to (d) the four different binding models (flavours) based on eqn (28) that can be used to describe a 1 : 2 equilibrium. The α-values are representative only as they do differ depending on the solvent used. Reproduced from ref. 26 with kind permission by the American Chemical Society.

ρ = 0.22 ($\Delta\Delta G_{coop}$ = −3.8 kJ mol^{-1}). The cooperativity observed is thought to originate from a combination of the favourable entropic effect and cooperative hydrogen-bonding effects in these aggregates. The results also readily explain why this compound forms gels in less competitive solvents.

The pathway complexity in the formation of a supramolecular polymer from a π-conjugated *S*-chiral oligo(*p*-phenylenevinylene) was studied using a combination of kinetic (stopped-flow) and temperature-dependent methods (Fig. 7b).[63] The kinetic experiment revealed that the metastable right-handed (*P*) helical aggregate is kinetically favoured over the thermodynamically stable left-handed (*M*) ones. While bearing some relation, the model used differs from the coEK model as it assumes that there are two phases; nucleation (here: a pentamer – n = 5), followed by a more favourable (cooperative) aggregation phase. In this particular work, the ratio of the nucleation/elongation equilibrium constants ($\approx\rho$) is 0.0525 for the stable *M*-helix but as the nucleation equilibrium constant for the *P*-helix is 1.38-times that for the *M*-helix, the metastable *P*-helix is the kinetically favoured product.[63]

7.2 Binding with a 1 : 2 stoichiometry

The example shown here (Fig. 8) illustrates how NMR titration methods can be used to evaluate thermodynamic parameters and equally importantly, whether the system is cooperative or not. In NMR titration experiments, 1 : 2 binding data are typically fitted to eqn (28):[7,8] if eqn (28) is used, four parameters have to be estimated in the fitting process. The question is whether it is always justifiable to use such a complex model to describe a 1 : 2 equilibrium. It is easy to envision that the binding is non-cooperative, and hence after using the relevant statistical factors σ, we obtain the following relation between the macroscopic binding constants: $K_1 = 4K_2$. Separately, we also need to consider if, in the current example, the NMR resonance changes are additive or not. If the two binding sites are far away from each other and there is very little structural communication between the sites, it makes sense that the NMR resonance changes are additive ($\delta_{\Delta HG_2} = 2\delta_{\Delta HG}$). In either scenario (non-cooperative binding model or additive NMR shift model), we need one parameter less in the data fitting process or if both effects combine (statistical 1 : 2 binding[7,8]), two parameters less are required.

This results in four (full, non-cooperative, additive and statistical) binding models (Fig. 8d). This is illustrated below in the binding of Ca^{2+} (Fig. 8a) and Cl^- (Fig. 8c) guests to a tetratopic ion-pair host.[26] The results show that positively charged ions such as calcium appear to bind with slightly negative or no cooperativity, whereas the anions including chloride show strong negative cooperativity. In the latter case with chloride, the data fit almost equally well to the full and additive flavour models (Fig. 8d) suggesting that binding at the first site has very little influence on the chemical environment of the second site (hence $\delta_{\Delta HG_2} = 2\delta_{\Delta HG}$). Interestingly, combining calcium and chloride ions (Fig. 8b) resulted in sigmoidal binding isotherms that are consistent with strong positive cooperativity, although the fit was too poor to accurately determine α. From DFT calculations, this positive cooperativity appears to have a $\Delta\Delta E$ in the order of 90 kcal mol^{-1}.[72]

To evaluate potential cooperativity in typical 1 : 2 (and 2 : 1) systems, an approach involving fitting the data to all four models and then systematically comparing the results, has recently be outlined in detail.[9] An online program for using these four different binding models for both NMR and UV-Vis titration data is readily available.[10]

7.3 Discrete di- and trivalent complexes and pseudorotaxanes

A common paradigm in supramolecular chemistry is that the best binders are perfectly preorganised and rigid. Rigidity is believed to reduce the entropic costs of binding, while a good geometric match is required to avoid enthalpically unfavourable strain upon complex formation. It is surprising that nature – in marked contrast to this notion – quite often prefers rather flexible spacers between binding sites in multivalent complexes. In recent studies of simple ammonium/crown ether complexes (Fig. 9),[73,74] chelate cooperativities have been determined for three series of flexible, semi-rigid and rigid divalent ammonium/crown complexes. Very clearly, the highest chelate cooperativities have been found for flexible spacers. In addition, flexible spacers can much better adapt to the steric requirements of the hosts than the more rigid analogues. Therefore, small deviations from the optimal geometry causes significant decreases in chelate cooperativity for rigid guests, while flexible guests maintain a rather high level of positive cooperativity even when their spacer length is quite far from the optimum. A precise analysis of chelate cooperativity factors can thus be helpful to define good design criteria for multivalent supramolecular hosts and guests. In contrast to common knowledge and in agreement with arguments also put forward by Whitesides *et al.*[11] and Hunter *et al.*,[75] flexible spacers may indeed be very helpful to achieve strong binding.

Increasing the size of the two crown ethers in the host to 24-crown-6 and the use of secondary ammonium ions allows synthesising (pseudo)rotaxanes with doubly (or triply) threaded geometries.[76,77] These pseudorotaxanes have been used to investigate the origin of chelate cooperativity in greater detail (Fig. 10).

In a series of divalent pseudorotaxanes, only the (semi-rigid) guest with the shortest spacer exhibits pronounced chelate cooperativity, while the addition of merely one methylene group completely destroys this effect. The crystal structure of the pseudorotaxane with the shortest guest reveals the origin of chelate cooperativity here: π-stacking interactions between the spacer of the host and the spacer of the guest result in additional binding energy. If one elongates the spacer by one or more methylene groups, the two phenyl rings of the guest spacer cannot be arranged similarly favourably anymore and thus, the additional spacer–spacer interactions are not operative anymore. This example very nicely demonstrates again, how strongly small mismatches in geometry affect chelate cooperativity in (semi-)rigid structures. It also reveals spacer–spacer interactions as a second origin of chelate cooperativity besides the rebinding effects discussed above.

Positive chelate cooperativity becomes a decisive factor, when efficient syntheses of multiply threaded interlocked molecules are concerned in order to generate functional molecules. The interaction between a naphthalenediimide (NDI) spacer in the axle and a tetrathiafulvalene (TTF) spacer in the crown ether host efficiently assembles a doubly threaded pseudorotaxane. This pseudorotaxane is then almost quantitatively converted into a pentastable redox-active doubly threaded rotaxane, in which the NDI acceptor and the TTF donor are fixed in close proximity.[78] Also, the photochromism of an azobenzene spacer in the axle of

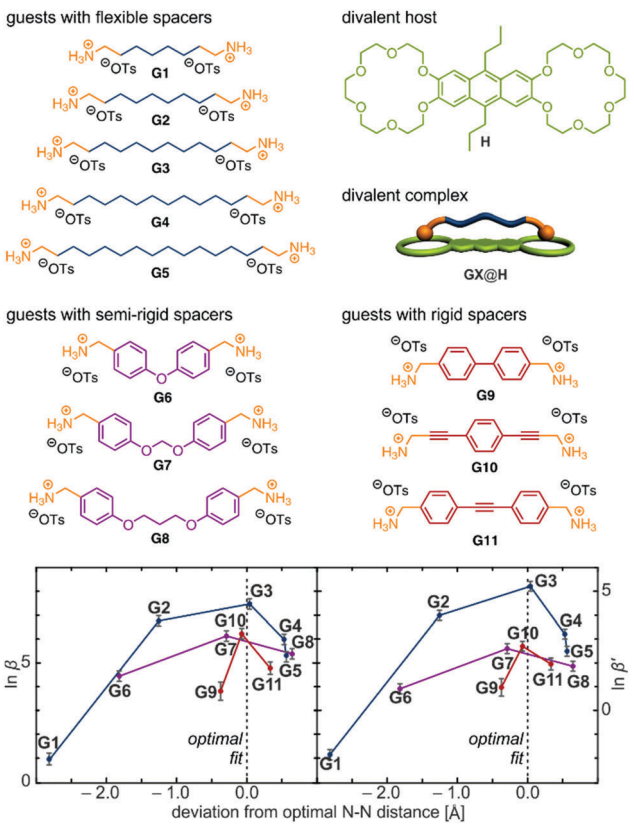

Fig. 9 Top: Structures of the three series of divalent flexible, semi-rigid and rigid guests, the divalent host and cartoon of the complex. Bottom: Plots of chelate cooperativity factors over the geometric fit. Clearly, guests with flexible spacers (dark blue lines) exhibit higher positive chelate cooperativity over a wider range of structures than guests with semi-rigid (violet lines) or with rigid (red lines) spacers. Adapted with permission from ref. 74.

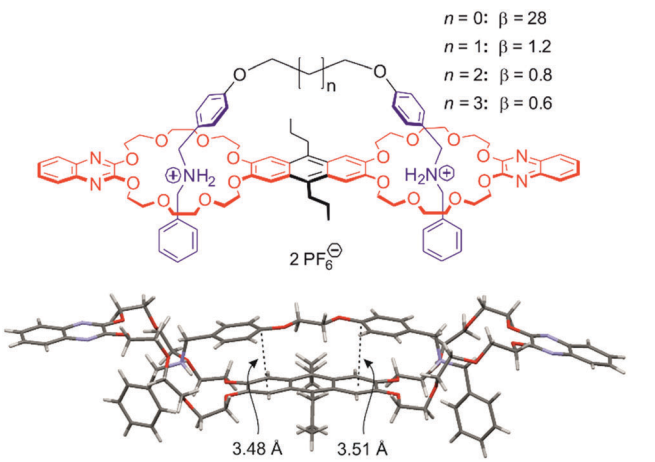

Fig. 10 Top: A remarkably pronounced effect of spacer length on chelate cooperativities is observed for this series of divalent pseudorotaxanes. Bottom: Crystal structure of the pseudorotaxane with the shortest guest spacer. Favourable spacer–spacer interactions account for the positive chelate cooperativity here.

a divalent pseudorotaxane can be switched on and off by acid/base-controlled pseudorotaxane formation.[79] A strongly positive chelate cooperativity with a high β value of 340 leads to the formation of a highly stable divalent pseudorotaxane, in which light-induced switching becomes impossible. Deprotonation of the secondary ammonium ions and subsequent dethreading of the axle enables photoswitching in this example of gated photochromism.

Besides ammonium/crown (pseudo)rotaxanes, amide (pseudo)-rotaxanes have also been investigated with respect to the chelate cooperativity effects.[80] Although the effects are usually smaller as compared to the ammonium/crown ether pseudorotaxanes, positive chelate cooperativity can significantly aid the synthesis. A triply threaded molecular elevator[81] has been assembled with almost quantitative yield even though the monovalent analogue only forms with *ca.* 70% yield. These examples clearly demonstrate how important a precise understanding of chelate cooperativity is for the design and synthesis of more complex and functional supramolecular structures.

7.4 Dissecting different non-covalent forces

After the discussion of di- and trivalent complexes bearing identical binding motifs (homomultivalent complexes), we now turn to examples showing that it is also possible to analyse heteromultivalent complexes, *i.e.* complexes in which the host and guest interact through different non-covalent interactions simultaneously. Applying the double mutant cycle analysis outlined above, it is then possible to dissect the overall binding into the contributions coming from each of the different non-covalent interactions.[82]

In an early study, Aoyama *et al.*[83] determined the contribution of hydrogen bonding to the overall binding energy of anthraquinone to a doubly naphthol-substituted porphyrin by applying the double mutant cycle approach (Fig. 11, top). Indeed, hydrogen bonding contributes -12.7 kJ mol^{-1} to the overall free binding energy of -13.5 kJ mol^{-1}. Consequently, π-stacking is by far the less important contribution to complex formation.

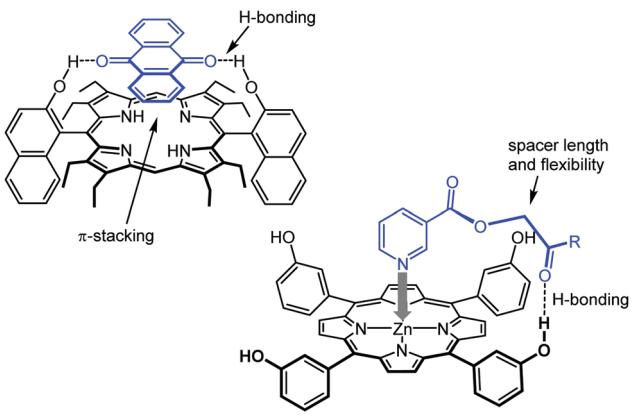

Fig. 11 Top: Aoyama's porphyrin platform, which allows designing double mutant cycles for the determination of the strength of hydrogen bonding *vs.* π-stacking. Bottom: Dissecting the individual interactions in Hunter's porphyrin–pyridine complexes allows not only determining the strength of hydrogen bonding in comparison to the total free interaction energy, but also studying structural effects of the spacers.

Such studies cannot only provide insight into the individual contributions of different interactions. By dissecting the different contributions to Zn porphyrin/pyridine complexes (Fig. 11, bottom), Hunter and co-workers were also able to uncover the structural effects of the spacers connecting the different binding sites on the binding energies. The effective molarities are significantly affected by conformational restriction,[84,85] and geometric complementarity,[86] while the intrinsic hydrogen bonding strength and solvent effects do not alter the EM values much.

7.5 Templated synthesis of large porphyrin wheels

In the last section, we discuss examples illustrating the power of multivalent binding for the creation of supramolecular architectures. Anderson *et al.* used an elegant template synthesis[87] for the preparation of giant, fully conjugated porphyrin wheels. As illustrated in Fig. 12 (top), zinc-containing porphyrins are the building blocks that finally form the giant macrocycles, while hexakis(pyridylphenyl)benzene acts as the template to pre-organise the linear porphyrin hexamer in a way suitable to induce cyclisation.

The five different effective molarities EM_1–EM_5 (Fig. 12, bottom) that describe the multivalent binding of the hexameric precursor to the template have been determined by double mutant cycle analyses using mono- to hexavalent template analogues and were compared to the EM values obtained for the corresponding

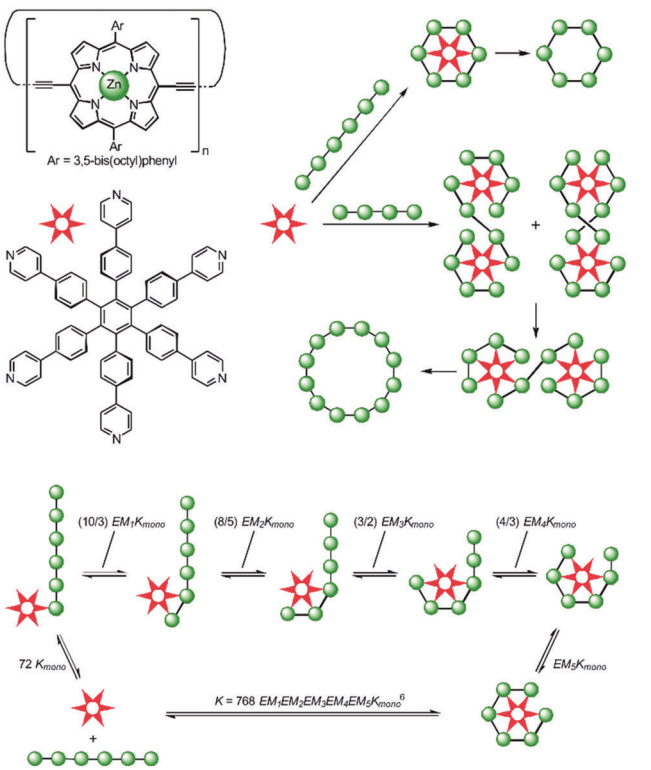

Fig. 12 Top: Elegant (Vernier) template-directed approaches to giant porphyrin wheels. Bottom: Detailed analysis of the multivalent interactions between a hexavalent template and a linear hexameric macrocyclisation precursor in terms of statistical factors, effective molarities and the monovalent binding constant.

binding of the cyclic product to the same templates.[88] While the third to sixth binding steps of the macrocycle reveals extreme effective molarities (up to 10^3 M), the linear hexameric precursor exhibits only moderate values (*ca.* 0.05 M). Nevertheless, the partially bound intermediates are not significantly populated and chelate cooperativity correspondingly aids in the macrocyclisation. As these macrocycles are fully conjugated systems, they exhibit particular properties:[89] a cyclic hexamer tetracation in its 4+ oxidation state is antiaromatic (80 π-electrons), while the 6+ oxidation state is aromatic (78 π-electrons), a behaviour which is connected to the special ring current effects.

This template approach has been extended to even larger porphyrin macrocycles by using Vernier templates, in which the number of binding sites of the template does not match that of the linear precursor. When a hexavalent template is combined with a linear tetramer, macrocyclisation results in a 12-mer macrocycle (Fig. 12, top),[90] as 12 is the lowest common multiple of 4 and 6. With larger, octavalent templates and linear decameric precursors, even 40-membered porphyrin wheels have been made.[91,92]

8 Conclusions

In the present review, we have summarised the different facets of cooperativity in supramolecular chemistry, which range from cooperative aggregation of supramolecular polymers and allosteric cooperativity in host–guest complexes with multivalent hosts and monovalent guests to chelate cooperativity in multivalent complexes and to the so far never investigated interannular cooperativity. For each type, we have provided the definitions of cooperativity factors and discussed how they relate to cooperativity-induced changes in free binding energy of two subsequent binding steps. Approaches for the thermodynamic analysis have been briefly introduced, most importantly the double mutant cycle analysis of chelate cooperativity.

In the past, the correct treatment of cooperativity has been under quite some debate. The discussion about the term "allosteric" is one example as the term itself implies – literally translated – that information on one binding event is transmitted to another binding site by structural changes. As this term might lead to misunderstandings, we suggest here that one may use "intermolecular cooperativity", if one does not intend to suggest a particular mechanism behind the cooperativity effect. As chelate cooperativity operates in the ring closure steps of multivalent complexes, we suggest using the term "intramolecular cooperativity" for consistency here.

The controversies over the correct definition of a chelate cooperativity factor is another example for the debates on cooperativity in the community. Both frequently used factors β and β' have advantages and disadvantages and have been criticised – β as it depends on the strength of the monovalent binding motif and β' as it is normalised to the total host concentration and a precise determination would therefore require often impracticably high host concentrations. Our own experience is that both factors result in very similar trends and in the same conclusions. Nevertheless, our recommendation is to calculate both. This can be done based on the same set of data and both factors can be compared easily to check whether it really makes a difference.

Multivalency and cooperativity are immensely important aspects of non-covalent binding as many self-assembled complexes would rather result in undefined polymeric networks rather than well-defined supramolecular architectures. In particular, when one wishes to design complex and functional supramolecular multi-component aggregates, a profound understanding of cooperativity effects will certainly contribute a significant share to our ability to plan how to construct them. The (few out of many) examples discussed at the end of our review illustrate that even seemingly simple intermolecular cooperative binding events can be complicated to analyse and how this can nevertheless be accomplished. Detailed thermodynamic analyses provide insight into the origins of intramolecular cooperativity – be they spacer–spacer interactions, rebinding effects or others. The individual contributions of different interactions can be dissected in order to unravel structural effects on the binding. This is again important to develop rules for the supramolecular design. They also show how cooperativity can contribute to the synthesis of immensely interesting yet complex molecular architectures.

Advances in this field will continue to be underpinned by studies aimed at formulating better models, dissecting the relative contributions of various non-covalent forces and electrostatic effects on cooperativity, and understanding how binding-induced changes to the dynamics of supramolecular systems influence cooperativity. The emerging field of far-from-equilibrium self-assembly within systems chemistry[93] is also likely to provide a fertile ground for new directions in the study of life-like cooperativity, especially given the importance of far-from-equilibrium in many biological cooperative systems including the ATP-driven aggregation of actin fibres in the cytoskeleton (Fig. 1).

Acknowledgements

We acknowledge the Australian Research Council for an ARC Centre of Excellence grant (CE140100036) to P. T. and the Deutsche Forschungsgemeinschaft for financial support to C. A. S. within the framework of the Cooperative Research Center (CRC 765) on multivalency. L. K. S. v. K. is grateful for a PhD fellowship awarded by the German Academic Scholarship Foundation.

Notes and references

1 C. Levinthal, in *Mössbauer Spectroscopy in Biological Systems*, ed. P. Debrunner, J. C. M. Tsibris and E. Münck, Univ. Illinois Press, Urbana, 1969, pp. 22–24.
2 B. Nagel, H. Dellweg and L. M. Gierasch, *Pure Appl. Chem.*, 1992, **64**, 143–168.
3 A. Whitty, *Nat. Chem. Biol.*, 2008, **4**, 435–439.
4 M. Takeuchi, M. Ikeda, A. Sugasaki and S. Shinkai, *Acc. Chem. Res.*, 2001, **34**, 865–873.

5 L. Kovbasyuk and R. Krämer, *Chem. Rev.*, 2004, **104**, 3161–3187.
6 A. J. Laos, J. C. Dean, Z. S. D. Toa, K. E. Wilk, G. D. Scholes, P. M. G. Curmi and P. Thordarson, *Angew. Chem., Int. Ed.*, 2017, DOI: 10.1002/anie.201607921.
7 P. Thordarson, *Chem. Soc. Rev.*, 2011, **40**, 1305–1323.
8 P. Thordarson, in *Supramolecular Chemistry: From Molecules to Nanomaterials*, ed. P. A. Gale and J. W. Steed, Wiley, Hoboken, 2012, vol. 2, pp. 239–274.
9 D. B. Hibbert and P. Thordarson, *Chem. Commun.*, 2016, **52**, 12792–12805.
10 http://supramolecular.org (accessed 12th January 2017).
11 M. Mammen, S.-K. Choi and G. M. Whitesides, *Angew. Chem., Int. Ed.*, 1998, **37**, 2754–2794.
12 C. Fasting, C. A. Schalley, M. Weber, O. Seitz, S. Hecht, B. Koksch, J. Dernedde, C. Graf, E.-W. Knapp and R. Haag, *Angew. Chem., Int. Ed.*, 2012, **51**, 10472–10498.
13 A. Mulder, J. Huskens and D. N. Reinhoudt, *Org. Biomol. Chem.*, 2004, **2**, 3409–3424.
14 J. D. Badjić, A. Nelson, S. J. Cantrill, W. B. Turnbull and J. F. Stoddart, *Acc. Chem. Res.*, 2005, **38**, 723–732.
15 H. Lee, Y.-H. Jeong, J.-H. Kim, I. Kim, E. Lee and W.-D. Jang, *J. Am. Chem. Soc.*, 2015, **137**, 12394–12399.
16 D. J. Diestler and E. W. Knapp, *J. Phys. Chem. C*, 2010, **114**, 5287–5304.
17 E. T. Mack, P. W. Snyder, R. Perez-Castillejos and G. M. Whitesides, *J. Am. Chem. Soc.*, 2011, **133**, 11701–11715.
18 M. Weber, A. Bujotzek and R. Haag, *J. Chem. Phys.*, 2012, **137**, 054111.
19 J. Monod, J. Wyman and J. P. Changeux, *J. Mol. Biol.*, 1965, **12**, 88–118.
20 D. E. Koshland, G. Nemethy and D. Filmer, *Biochemistry*, 1966, **5**, 365–385.
21 A. Cooper and D. T. F. Dryden, *Eur. Biophys. J.*, 1984, **11**, 103–109.
22 C.-J. Tsai, A. del Sol and R. Nussinov, *Mol. BioSyst.*, 2009, **5**, 207–216.
23 L. R. Otterbein, P. Graceffa and R. Dominguez, *Science*, 2001, **293**, 708–711.
24 J. Rebek, Jr., T. Costello, L. Marshall, R. Wattley, R. C. Gadwood and K. Onan, *J. Am. Chem. Soc.*, 1985, **107**, 7481–7487.
25 C. A. Hunter and H. L. Anderson, *Angew. Chem., Int. Ed.*, 2009, **48**, 7488–7499.
26 E. N. W. Howe, M. Bhadbhade and P. Thordarson, *J. Am. Chem. Soc.*, 2014, **136**, 7505–7516.
27 G. Ercolani and L. Schiaffino, *Angew. Chem., Int. Ed.*, 2011, **50**, 1762–1768.
28 T. F. A. De Greef, M. M. J. Smulders, M. Wolffs, A. P. H. J. Schenning, R. P. Sijbesma and E. W. Meijer, *Chem. Rev.*, 2009, **109**, 5687–5754.
29 C. Kulkarni, S. Balasubramanian and S. J. George, *ChemPhysChem*, 2013, **14**, 661–673.
30 P. Besenius, *J. Polym. Sci., Part A: Polym. Chem.*, 2017, **55**, 34–78.
31 R. B. Martin, *Chem. Rev.*, 1996, **96**, 3043–3064.
32 G. Ercolani, C. Piguet, M. Borkovec and J. Hamacek, *J. Phys. Chem. B*, 2007, **111**, 12195–12203.
33 G. Ercolani, *Chem. Commun.*, 2001, 1416–1417.
34 M. P. Evstigneev, A. S. Buchelnikov, V. V. Kostjukov, I. S. Pahskova and V. P. Evstigneeev, *Supramol. Chem.*, 2013, **25**, 199–203.
35 N. J. Buurma and I. Haq, *J. Mol. Biol.*, 2008, **381**, 607–621.
36 P. van der Schoot, in *Supramolecular Polymers*, ed. A. Ciferri, CRC Press, Baton Rouge, 2nd edn, 2005, pp. 77–106.
37 P. Jonkheijm, P. van der Schoot, A. P. H. J. Schenning and E. W. Meijer, *Science*, 2006, **313**, 80–83.
38 M. P. Evstigneev, *Int. Rev. Phys. Chem.*, 2014, **33**, 229–273.
39 K. Nakamoto, T. Tsubio and G. D. Strahan, *Drug-DNA Interactions: Structures and Spectra*, Wiley, Hoboken, 2008.
40 D. Hörter and J. B. Dressman, *Adv. Drug Delivery Rev.*, 2001, **46**, 75–87.
41 M. P. Evstigneev, D. B. Davies and A. N. Veselkov, *Chem. Phys.*, 2006, **321**, 25–33.
42 A. J. Markvoort, H. M. M. ten Eikelder, P. A. J. Hilbers, T. F. A. de Greef and E. W. Meijer, *Nat. Commun.*, 2011, **2**, 509.
43 H. M. M. ten Eikelder, A. J. Markvoort, T. F. A. de Greef and E. W. Meijer, *J. Phys. Chem. B*, 2012, **116**, 5291–5301.
44 S. Shinkai, M. Ikeda, A. Sugasaki and M. Takeuchi, *Acc. Chem. Res.*, 2001, **34**, 494–503.
45 C. Kremer and A. Lützen, *Chem. – Eur. J.*, 2013, **19**, 6162–6196.
46 M. F. Perutz, *Q. Rev. Biophys.*, 1989, **22**, 139–236.
47 D. M. Bishop and K. J. Laidler, *J. Chem. Phys.*, 1965, **42**, 1688–1691.
48 S. W. Benson, *J. Am. Chem. Soc.*, 1958, **80**, 5151–5154.
49 R. Cacciapaglia, S. Di Stefano and L. Mandolini, *Acc. Chem. Res.*, 2004, **37**, 113–122.
50 M. J. Mayoral, N. Bilbao and D. González-Rodríguez, *ChemistryOpen*, 2016, **5**, 10–32.
51 J. Hamacek, Self-Assembly Principles of Helicates, in *Metallofoldamers*, ed. G. Maayan and M. Albrecht, Wiley, Hoboken/USA, 2013.
52 J. Hamacek, M. Borkovec and C. Piguet, *Chem. – Eur. J.*, 2005, **11**, 5217–5226.
53 J. Hamacek, M. Borkovec and C. Piguet, *Chem. – Eur. J.*, 2005, **11**, 5227–5237.
54 W. P. Jencks, *Proc. Natl. Acad. Sci. U. S. A.*, 1981, **88**, 4046–4050.
55 A. Camara-Campos, D. Musumeci, C. A. Hunter and S. Turega, *J. Am. Chem. Soc.*, 2009, **131**, 18518–18524.
56 G. S. Wilson and H. L. Anderson, *Chem. Commun.*, 1999, 1539–1540.
57 M. Takeuchi, M. Ikeda, A. Sugasaki and S. Shinkai, *Acc. Chem. Res.*, 2001, **34**, 865–873.
58 G. Ercolani, *Org. Lett.*, 2005, **7**, 803–805.
59 P. Thordarson, E. J. A. Bijsterveld, J. A. A. W. Elemans, P. Kasák, R. J. M. Nolte and A. E. Rowan, *J. Am. Chem. Soc.*, 2003, **125**, 1186–1187.
60 A. J. Lowe, F. Pfeffer and P. Thordarson, *Supramol. Chem.*, 2012, **24**, 585–594.
61 P. N. Taylor and H. L. Anderson, *J. Am. Chem. Soc.*, 1999, **121**, 11538–11545.

62 C. A. Hunter, M. C. Misuraca and S. M. Turega, *Chem. Sci.*, 2012, **3**, 589–601.
63 P. A. Korevaar, S. J. George, A. J. Markvoort, M. M. J. Smulders, P. A. J. Hilbers, A. P. H. J. Schenning, T. F. A. De Greef and E. W. Meijer, *Nature*, 2012, **481**, 492–496.
64 P. G. A. Janssen, P. Jonkheijm, P. Thordarson, J. L. J. van Dongen, E. W. Meijer and A. P. H. J. Schennings, *J. Mater. Chem.*, 2007, **17**, 2654–2660.
65 F. P. Schmidtchen, in *Analytical Methods in Supramolecular Chemistry*, ed. C. A. Schalley, Wiley-VCH, Weinheim, 2nd edn, 2012, vol. 1, pp. 67–104.
66 G. A. Holdgate, *BioTechniques*, 2001, **31**, 164–184.
67 A. Arnaud and L. Bouteiller, *Langmuir*, 2004, **20**, 6858–6863.
68 Principles and Practice, in *Handbook of Thermal Analysis and Calorimetry*, ed. M. E. Brown, Elsevier Science B.V., Amsterdam, 1998, vol. 1.
69 T. Wiseman, S. Williston, J. F. Brandts and L.-N. Lin, *Anal. Biochem.*, 1989, **179**, 131–137.
70 W. B. Turnbull and A. H. Daranas, *J. Am. Chem. Soc.*, 2003, **125**, 14859–14866.
71 J. E. A. Webb, M. J. Crossley, P. Turner and P. Thordarson, *J. Am. Chem. Soc.*, 2007, **129**, 7155–7162.
72 E. N. W. Howe, G. E. Ball and P. Thordarson, *Supramol. Chem.*, 2015, **27**, 829–839.
73 L. K. S. von Krbek, A. J. Achazi, M. Solleder, M. Weber, B. Paulus and C. A. Schalley, *Chem. – Eur. J.*, 2016, **22**, 15475–15484.
74 L. K. S. von Krbek, A. J. Achazi, S. Schoder, M. Gaedke, T. Biberger, B. Paulus and C. A. Schalley, *Chem. – Eur. J.*, 2017, **23**, 2877–2883.
75 H. Sun, C. A. Hunter and E. M. Llamas, *Chem. Sci.*, 2015, **6**, 1444–1453.
76 W. Jiang, K. Nowosinski, N. L. Löw, E. V. Dzyuba, F. Klautzsch, A. Schäfer, J. Huuskonen, K. Rissanen and C. A. Schalley, *J. Am. Chem. Soc.*, 2012, **134**, 1860–1868.
77 K. Nowosinski, L. K. S. von Krbek, N. L. Traulsen and C. A. Schalley, *Org. Lett.*, 2015, **17**, 5076–5079.
78 H. V. Schröder, H. Hupatz, A. J. Achazi, S. Sobottka, B. Sarkar, B. Paulus and C. A. Schalley, *Chem. – Eur. J.*, 2017, **23**, 2960–2967.
79 M. Lohse, K. Nowosinski, N. L. Traulsen, A. J. Achazi, L. K. S. von Krbek, B. Paulus, C. A. Schalley and S. Hecht, *Chem. Commun.*, 2015, **51**, 9777–9780.
80 N. L. Traulsen, C. H.-H. Traulsen, P. M. Deutinger, S. Müller, D. Schmidt, I. Linder and C. A. Schalley, *Org. Biomol. Chem.*, 2015, **13**, 10881–10887.
81 L. Kaufmann, N. L. Traulsen, A. Springer, H. V. Schröder, T. Mäkelä, K. Rissanen and C. A. Schalley, *Org. Chem. Front.*, 2014, **1**, 521–531.
82 S. L. Cockroft and C. A. Hunter, *Chem. Soc. Rev.*, 2007, **36**, 172–188.
83 Y. Aoyama, M. Asakawa, Y. Matsui and H. Ogoshi, *J. Am. Chem. Soc.*, 1991, **113**, 6233–6240.
84 H. Adams, E. Chekmeneva, C. A. Hunter, M. C. Misuraca, C. Navarro and S. M. Turega, *J. Am. Chem. Soc.*, 2013, **135**, 1853–1863.
85 H. Sun, K. Guo, H. Gan, X. Li and C. A. Hunter, *Org. Biomol. Chem.*, 2015, **13**, 8053–8066.
86 H. Sun, C. A. Hunter, C. Navarro and S. Turega, *J. Am. Chem. Soc.*, 2013, **135**, 13129–13141.
87 J. K. Sprafke, B. Odell, T. D. W. Claridge and H. L. Anderson, *Angew. Chem., Int. Ed.*, 2011, **50**, 5572–5575.
88 H. J. Hogben, J. K. Sprafke, M. Hoffmann, M. Pawlicki and H. L. Anderson, *J. Am. Chem. Soc.*, 2011, **133**, 20962–20969.
89 M. D. Peeks, T. D. W. Claridge and H. L. Anderson, *Nature*, 2017, **541**, 200–203.
90 D. V. Kondratuk, J. K. Sprafke, M. C. O'Sullivan, L. M. A. Perdigão, A. Saywell, M. Malfois, J. N. O'Shea, P. H. Beton and H. L. Anderson, *Chem. – Eur. J.*, 2014, **20**, 12826–12834.
91 D. V. Kondratuk, L. M. A. Perdigão, M. C. O'Sullivan, S. Svatek, G. Smith, J. N. O'Shea, P. H. Beton and H. L. Anderson, *Angew. Chem., Int. Ed.*, 2012, **51**, 6696–6699.
92 D. V. Kondratuk, L. M. A. Perdigão, A. M. S. Esmail, J. N. O'Shea, P. H. Beton and H. L. Anderson, *Nat. Chem.*, 2015, **7**, 317–322.
93 E. Mattia and S. Otto, *Nat. Nanotechnol.*, 2015, **10**, 111–119.